

COLLISION-BASED DYNAMICS FOR MULTI-MARGINAL OPTIMAL TRANSPORT

Mohsen Sadr and Hossein Gorji

ABSTRACT. Inspired by the Boltzmann kinetics, we propose a collision-based dynamics with a Monte Carlo solution algorithm that approximates the solution of the multi-marginal optimal transport problem via randomized pairwise swapping of sample indices. The computational complexity and memory usage of the proposed method scale linearly with the number of samples, making it highly attractive for high-dimensional settings. In several examples, we demonstrate the efficiency of the proposed method compared to the state-of-the-art methods.

1. INTRODUCTION

Since its introduction by Gaspard Monge [1] and seminal contributions by Leonid Kantorovich [2], the Optimal Transport (OT) has evolved into a rich mathematical framework with fruitful theoretical properties. At its core, it gives a geometrically intuitive basis to compare and interpolate probability distributions, leading to wide-range of applications across many fields. This includes interpolation between images [3], clustering dataset [4], surrogate models [5], calibration of stochastic processes [6], and finding the N-body particle distribution function in density functional theory [7]. However, the computational complexity associated with the underlying optimization problem limits the use of OT in large datasets. This is due to the fact that the OT problem is inherently linear programming over an infinite-dimensional space, resulting in computationally intensive optimization. The problem can even become intractable if multi-marginals are considered. Though non-exclusively, we can categorize the main computational algorithms for numerical solution to the OT problem as the following.

Linear programming. This is the direct approach in solving the OT problem, also known as Earth Mover’s Distance in the literature [8]. Linear programming has been applied mainly to the two-marginal OT problem, where the computational complexity becomes $\mathcal{O}(N_p^3 \log(N_p))$ for N_p number of samples per marginal. Fast EMD algorithms use the network simplex with empirical computational complexity of $\mathcal{O}(N_p^2)$ [9].

Regularization via entropy. By incorporating entropy in the cost functional of the two-marginal OT, one derives a relaxed version of the OT problem [10, 11]. The resulting optimization problem is convex and can be solved efficiently using the so-called Sinkhorn method, with the computational

Date: December 24, 2024.

Emails: mohsen.sadr@psi.ch, mohammadhossein.gorji@empa.ch

Mohsen Sadr: Paul Scherrer Institute, Forschungsstrasse 111, CH-5232 Villigen, Switzerland. Hossein Gorji: Laboratory for Computational Engineering, Empa, Dübendorf, Switzerland.

complexity of $\mathcal{O}(N_p^2)$.

Dynamic processes. Optimal maps can be described by dynamic processes. For example, the fluid dynamic formulation, given by Benamou-Brenier dynamics, describes the OT problem in the form of the Hamilton-Jacobi dynamics [12]. Another class of dynamic formulation is given by marginal preserving processes, where OT (and its entropy regularized version) is recovered at the stationary state [13]. In particular, Orthogonal Coupling Dynamics [14] introduces an efficient algorithm with the computational complexity of $\mathcal{O}(N_p \log(N_p))$.

Reduction to assignment problem. As shown by [15], OT in discrete setting is closely related to the assignment problem. A notably efficient approximate solution is introduced by Iterative Swapping Algorithm (ISA) [16, 17], where a near-optimal permutation of discrete points is found via consecutive swaps of samples in each marginal. The ISA has the computational complexity of $\mathcal{O}(N_p^2)$, and is the closest method to what we develop here.

Other notable approximate methods include moment-based methods [18, 19], simulated annealing [20], and sliced-Wasserstein [21, 22].

Contributions. We focus on the multi-marginal OT problem in the discrete setting, where only samples of the marginals are provided. Unlike the optimal assignment approach, which looks for the optimal permutation of samples, we iteratively improve the permutation of samples by pair-wise swapping. Instead of checking all possible swaps, which is pursued in ISA, we devise a random algorithm inspired by Boltzmann kinetics, where binary collisions are performed by randomly selecting collision pairs. We formalize both ISA and our collision-based algorithm, and motivate their consistency.

We show that in the case of the OT problem with L^p -transport cost, the complexity of checking the condition for a swap to be accepted/rejected is independent of number of samples. Furthermore, we show that the complexity of the collision-based method scales linearly with number of samples. We empirically investigate its convergence behaviour and observe exponential convergence to the stationary solution, regardless of number of samples/marginals/dimension. In several toy examples, we show the error and performance of the proposed method compared to Sinkhorn and EMD. Then, as a show case, we assess the flexibility of the method in finding the optimal map in a five-marginal problem, which allows us to learn a map between normal and other target densities. As an application in Machine Learning, we demonstrate the performance of collision-based method in finding the distribution of the Wasserstein distance in the Japanese female facial expression and butterfly datasets.

Definitions, Notations, and Problem Setup. Let $\mathcal{P}(\mathcal{X}_i)$ be the space of non-negative Borel measures over $\mathcal{X}_i \subset \mathbb{R}^n$, and

$$\mathcal{P}_2(\mathcal{X}_i) := \left\{ \mu \in \mathcal{P}(\mathcal{X}_i) \mid \int_{\mathcal{X}_i} \|x\|_2^2 \mu(dx) < \infty \right\} \quad (1)$$

with $\|\cdot\|_2$ the usual L^2 -Euclidean norm. Consider K probability measures $\mu_i \in \mathcal{P}_2(\mathcal{X}_i)$ with $i \in \{1, \dots, K\}$, and vanishing on $(n-1)$ -rectifiable sets [23]. We are interested in the Multi-Marginal

Optimal Transport problem (MMOT), which seeks the minimization

$$\pi_{\text{opt}} := \arg \min_{\pi \in \Pi(\mu_1, \dots, \mu_K)} \int_{\mathcal{X}} c(x_1, \dots, x_K) \pi(dx), \quad (2)$$

where \mathcal{X} is the product set $\mathcal{X} := \mathcal{X}_1 \times \dots \times \mathcal{X}_K$. The optimization is constrained on Π , which is the set of coupling measures

$$\Pi(\mu_1, \dots, \mu_K) := \left\{ \pi \in \mathcal{P}_2(\mathcal{X}) \mid \text{proj}_i(\pi) = \mu_i \ \forall i \in \{1, \dots, K\} \right\} \quad (3)$$

and $\text{proj}_i : \mathcal{X} \rightarrow \mathcal{X}_i$ is the canonical projection. In order for MMOT to have a solution, it is sufficient to assume that the cost $c : \mathcal{X} \rightarrow \mathbb{R}$ is lower-semicontinuous [23]. In general there is no guarantee that the optimal transport plan, i.e. π_{opt} , is induced by an optimal map. The existence of the optimal map entails further constraints on the cost. One interesting setting, which has been analyzed thoroughly, is when $K = 2$ and $c(x_1, x_2) = \|x_1 - x_2\|_2^2$. For this L^2 -OT setting, the optimal map exists and is unique [24, 25]. The generalization of L^2 -OT to MMOT has been carried out by the seminal work of Gangbo and Swiech [23]. Consider

$$c(x_1, \dots, x_K) = \sum_{i=1}^K \sum_{j=i+1}^K \frac{1}{2} \|x_i - x_j\|_2^2, \quad (4)$$

the optimal plan π_{opt} then takes a deterministic form and is concentrated on optimal maps. In fact, the equivalent form of (2) is given by optimization over the maps $\{T_i\} \in \mathcal{T}_K$, where

$$\mathcal{T}_K := \{T = \{T_i\}_{i=1, \dots, K} \mid T_i : \mathcal{X}_1 \rightarrow \mathcal{X}_i, T_i \# \mu_1 = \mu_i, T_1 = \text{id}\} \quad (5)$$

such that

$$\inf \left\{ \int_{\mathcal{X}_1} \sum_{i=1}^K \sum_{j=i+1}^K \frac{1}{2} \|T_i(x_1) - T_j(x_1)\|_2^2 \mu_1(dx_1) \mid \{T_i\}_{i=1, \dots, K} \in \mathcal{T}_K \right\} \quad (6)$$

is attained [26, 23]. Though our devised algorithm is not restricted to a specific choice of $c(\cdot)$, in order to keep the study focused, we target the Gangbo-Swiech setting and refer to it as L^2 -MMOT problem. It is clear that the setting reduces to L^2 -OT for $K = 2$. We refer the reader to [27] and references therein for detailed analysis of existence and uniqueness in MMOT problem.

Instead of direct access to $\{\mu_i\}$, we consider the scenario where only N_p independent samples of each marginal, i.e. $\hat{X}^{(i)} = \{\hat{X}_1^{(i)}, \dots, \hat{X}_{N_p}^{(i)}\} \sim \mu_i$, is known. Given $\{\hat{X}^{(i)}\}$ for $i \in \{1, \dots, K\}$, the pursued algorithm seeks to find estimates of π_{opt} along with the corresponding optimal maps $\{T_i\}$. In particular, let $(X_t^{(i)})_{t \geq 0} : \Omega \rightarrow \mathcal{X}_i$ be a Markov process on the sample space Ω , which is initialized by $\hat{X}^{(i)}$ and belongs to the Hilbert space $\mathcal{H} = \mathcal{L}^2(\Omega, \mathcal{F}_t, \mathbb{P}^{(i)})$. The latter is the space of square-integrable functions, which map Ω to \mathcal{X}_i and are \mathcal{F}_t -measurable at time t , with the probability function $\mathbb{P}^{(i)}$. Our plan is to devise a process such that $\hat{\pi}_t = 1/N_p \sum_{i=1}^{N_p} \delta_{X_{i,t}^{(1)}, \dots, X_{i,t}^{(K)}}$ approximates π_{opt} as t becomes large. As a by-product, the samples of the process will be regressed to recover the maps $\{T_i\}$. We denote by $\tilde{\pi}_t^{X_i^{(s)} \leftrightarrow X_j^{(s)}}$ the empirical joint measure $\tilde{\pi}_t$ updated by the sample swap between $X_i^{(s)}$ and $X_j^{(s)}$ of marginal s .

2. MAIN IDEA

Given independent and identically distributed (i.i.d.) samples $\{\hat{X}^{(i)}\}$, we develop a stochastic update rule that guides the resulting realizations toward approximating the optimal solution of (2). Our objective is to construct this update rule in such a way that the computational complexity of each iteration scales linearly with the number of samples. A natural representation of the distribution based on given samples is via empirical measure

$$\tilde{\mu}_i = \frac{1}{N_p} \sum_{j=1}^{N_p} \delta_{\hat{X}_j^{(i)}}. \quad (7)$$

We leverage several key ideas in order to proceed. Let us focus on two marginal setup, i.e. $K = 2$, and recall the following facts [28, 29, 30].

- (1) For discrete measures of the form (7), the optimal cost is given by

$$\min_{\pi \in \Pi(\tilde{\mu}_1, \tilde{\mu}_2)} \int c(x_1, x_2) \pi(dx) = \min_{\gamma \in B^{N_p}} \frac{1}{N_p} \sum_{i,j} c(\hat{X}_i^{(1)}, \hat{X}_j^{(2)}) \gamma_{ij} \quad (8)$$

where B^{N_p} is the set of $N_p \times N_p$ bistochastic matrices.

- (2) The extremal points of B^{N_p} are permutation matrices. Therefore

$$\tilde{\pi}^{\text{opt}} = \min_{\sigma \in \Sigma^{N_p}} \frac{1}{N_p} \sum_{i=1}^{N_p} \delta_{(\hat{X}_i^{(1)}, \hat{X}_{\sigma(i)}^{(2)})} \quad (9)$$

where Σ^{N_p} is the set of permutations of $\{1, \dots, N_p\}$. The corresponding optimal map is given by $\tilde{T}(\hat{X}_i^{(1)}) = \hat{X}_{\sigma^{\text{opt}}(i)}^{(2)}$.

- (3) For the L^2 cost, as $N_p \rightarrow \infty$, the optimal distribution and map weakly converge to the solution of the Monge-Kantorovich problem, i.e. $(\tilde{\pi}^{\text{opt}}, \tilde{T}) \rightharpoonup (\pi^{\text{opt}}, T)$.

Hence the equivalent form of optimization problem (2), admitting the mentioned assumptions, is given by a search over permutation matrices. In general, this remains a computationally intensive task, see e.g. the Hungarian algorithm [31]. To address this, a nested approach for finding a nearly optimal permutation matrix was proposed in [16, 17]. The Iterative Swapping Algorithm (ISA) aims to identify a near-optimal permutation by performing pairwise index swaps that reduce the cost. However, because ISA examines all possible swaps, its computational complexity remains quadratic.

Starting from the premise that pairwise index swapping can yield near-optimal permutations, we introduce a stochastic variant of the ISA by drawing on analogies with Boltzmann kinetics. Rather than exhaustively examining all possible pairwise swaps, our approach involves randomly grouping indices, with each group containing only one swapping pair. Therefore at each iteration, only $N_p/2$ swapping candidates are assessed (instead of $N_p(N_p - 1)/2$ required in ISA). This reduction simplifies the complexity of our stochastic version to linear scaling with respect to N_p .

Our scheme draws a close analogy to Boltzmann kinetics, and it is helpful to introduce the concept of particles to clarify this setup. Each particle represents a realization of a random variable, sampled from a marginal distribution. In this context, swapping can be viewed as a binary collision

event. If accepted, the collision results in an index swap between two collision pairs. While a brute-force approach requires $N_p(N_p - 1)/2$ collision pairs to be checked at every iteration, Bird [32] introduced a randomization technique that requires only $N_p/2$ collision pairs to be considered, without introducing bias—as long as the selection of collision pairs is independent of the collision updates. This randomization concept has since been extended in fields such as stochastic gradient descent and mini-batch molecular dynamics.

Building on these insights, we review ISA and present collision-based dynamics, followed by a heuristic Boltzmann-like kinetic equation.

3. PROCESS FORMULATIONS

Consider discrete time index $t \in \{0, 1, \dots\}$ and i.i.d. samples $\hat{X}_j^{(i)}$ for marginal i and sample index $j = 1, \dots, N_p$.

- (1) *ISA process:* For each marginal $i \in \{1, \dots, K\}$ and samples $j, k \in \{1, \dots, N_p\}$ with $k \geq j$, ISA updates the samples via

$$(X_{j,t+1}^{(i)}, X_{k,t+1}^{(i)})^T = \mathcal{K}_{j,k}(X_{j,t}^{(i)}, X_{k,t}^{(i)})^T. \quad (10)$$

The swaps are guided by the discrete cost

$$m(\tilde{\pi}_t) = \mathbb{E}_{\tilde{\pi}_t}[c] \quad (11)$$

where $\tilde{\pi}_t$ is the empirical measure of X_t . The swapping kernel is given by

$$\mathcal{K}_{j,k} = \begin{cases} I_{2n \times 2n} & \text{if } m(\tilde{\pi}_t^{X_j^{(i)} \leftrightarrow X_k^{(i)}}) \geq m(\tilde{\pi}_t) \\ J_{2n \times 2n} & \text{if } m(\tilde{\pi}_t^{X_j^{(i)} \leftrightarrow X_k^{(i)}}) < m(\tilde{\pi}_t) \end{cases} \quad (12)$$

with $I_{n \times n}$ as the identity matrix and J an exchange matrix of the form

$$J_{2n \times 2n} = \begin{bmatrix} 0_{n \times n} & I_{n \times n} \\ I_{n \times n} & 0_{n \times n} \end{bmatrix} \quad (13)$$

and $0_{n \times n}$ is a $n \times n$ matrix with zero entries. The swapping kernel (12) allows swaps if it leads to reduction in the cost associated with the empirical measure (11).

- (2) *Collision-based dynamics:* The proposed collision-based version of ISA performs similar steps with the difference that j, k are now chosen from a random subset $\mathcal{C} \subset \{1, \dots, N_p\}$ of size 2. Therefore in collision-based method, instead of applying (10) to all pairs $k, j \in \{1, \dots, N_p\}$ with $k \geq j$, we pick $j, k \sim \mathcal{U}([1, N_p])$ where $\mathcal{U}(\cdot)$ is a discrete uniform measure with values between 1 and N_p . As a result, the complexity of the algorithm reduces to $\mathcal{O}(N_p)$. Note that this randomization step in general can be justified as long as the subsets are sampled independent of the random variable X . While the consistency proofs exist for range of kernels [33], we leave the theoretical justification of the consistency between collision-based process and ISA to separate studies.

- (3) *Boltzmann kinetics*: There is a close analogy between the proposed collision process and Boltzmann kinetics. To simplify the illustration, let us consider a setup of two marginals $\{\mu_1, \mu_2\}$. The proposed collision process evolves an initial joint measure of $\{\mu_1, \mu_2\}$ in a fashion similar to binary collisions, where collisions refer to swapping the state of two particles. Given that the collision here simply exchanges the sample values, the equivalent Boltzmann operator takes a concise form. Let ρ_t be the time dependent density of the joint measure and fix $\tau > 0$ as a collision time scale. An equivalent collision operator of the Boltzmann-type can be described as

$$Q[\rho_t, \rho_t] = \frac{1}{\tau} \int_{\mathbb{R}^{2n}} \left(\rho_t(x_1, y) \rho_t(x, y_1) - \rho_t(x, y) \rho_t(x_1, y_1) \right) \Omega(x, x_1, y, y_1) dx_1 dy_1, \quad (14)$$

where the collision kernel reads

$$\Omega(x, x_1, y, y_1) = H\left(c(x, y) + c(x_1, y_1) - c(x_1, y) - c(x, y_1)\right) \quad (15)$$

and $H(\cdot)$ is the Heaviside function. Heuristically, the kinetic model (14) describes a process where binary collisions are only accepted if the cost c is decreased by the swaps between the two randomly picked sample points. However, one should note that the Boltzmann kinetics operate on the continuous time whereas the proposed collision process is discrete in time. Although consistency between the two descriptions may be proven following the recipe provided by Wagner's proof of Monte Carlo solution to the Boltzmann equation [34], we leave out the theoretical justifications for future works.

4. MONTE CARLO SOLUTION ALGORITHM FOR THE COLLISIONAL DYNAMICS

Motivated by the direct Monte Carlo solution algorithms to the Boltzmann [35] and the Fokker-Planck equation [36] for rarefied gas and plasma dynamics, here we devise a collision-based numerical scheme to solve the discrete optimal transport problem. In order to ensure that all the particles are considered for the collision in one time step, we consider the following collision routine for each marginal:

- Generate a random list of particle indices R of size N_p without repetition.
- Decompose R into two subsets of the same size I and J where $I \cap J = \emptyset$.
- Swap particles with indices I_k and J_k for collisions using (10) where $k = 1, \dots, N_p/2$.

We note that by shuffling the particle indices, one can easily find a random list of particle indices R . In Algorithm 1, we give a detailed description of the proposed method.

5. PROPERTIES OF COLLISIONAL DYNAMICS FOR THE OPTIMAL TRANSPORT PROBLEM

The proposed collision-based Monte Carlo solution Algorithm 1 has several numerical properties that we list next.

- **Marginal preservation.** Since we only change the order of particles in each marginal when a collision is accepted, Algorithm 1 preserves the marginals up to machine accuracy on the discrete points.

Algorithm 1: Collision-based algorithm to MMOT problem**Input:** $X := [X^{(1)}, \dots, X^{(K)}]$ and tolerance $\hat{\epsilon}$ # $\dim(X) = K \times N_p \times n$ **repeat** **for** $i = 1, \dots, K$ **do** Generate an even-size random list of particle indices R ; Decompose R into same-size subsets I and J where $I \cap J = \emptyset$ and $|I| = |J| = \lfloor N_p/2 \rfloor$; **for** $k = 1, \dots, \lfloor N_p/2 \rfloor$ **do** **if** $m(\hat{\pi}_t^{X_{I_k}^{(i)} \leftrightarrow X_{J_k}^{(i)}}) < m(\hat{\pi}_t)$ **then** # Accept the collision and update X ; $X_{I_k}^{(i)} \leftarrow X_{J_k}^{(i)}$ and $X_{J_k}^{(i)} \leftarrow X_{I_k}^{(i)}$; **end** **end** **end****until** Convergence in $\mathbb{E}_{\hat{\pi}_t}[c(X_t^{(1)}, \dots, X_t^{(K)})]$ with tolerance $\hat{\epsilon}$;**Output:** X

- **Monotone convergence.** Collisions are only accepted if they reduce the cost of the optimal transport problem. This guarantees that Algorithm 1 converges to the stationary solution monotonically. However, finding the convergence rate is not trivial given the discontinuity of the jump process.

If the proposed collision-based dynamics behaves similar to the Boltzmann kinetics, we expect that the proposed Algorithm 1 converges exponentially to its stationary solution. In particular, we expect that $\hat{\pi}$ exponentially converges to optimal $\hat{\pi}_{\text{opt}}$, i.e. the error $\epsilon := |(\hat{\pi}(t) - \hat{\pi}_{\text{opt}})/(\hat{\pi}(0) - \hat{\pi}_{\text{opt}})|$ follows

$$\epsilon = \mathcal{O}(e^{-\alpha t}) \quad (16)$$

where α denotes the ratio of accepted collisions per number of candidates. However, after a short transition, we expect the algorithm to become stiff as the probability of finding new acceptable collision pairs reduces quickly, i.e. $\alpha \rightarrow 0$ as $\hat{\pi} \rightarrow \hat{\pi}_{\text{opt}}$. Therefore, the proposed algorithm converges exponentially to a sub-optimal solution $\hat{\pi}_{\text{sub-opt}}$ as long as α remains large. In the numerical tests presented in 6, we show in several examples that the recovered sub-optimal solution has a reasonably small relative error compared to EMD, making it useful for practical purposes.

- **Affordable computational complexity.** Each iteration of Algorithm 1 for a given marginal has the computational complexity of $\mathcal{O}(\beta N_p)$ where β denotes the cost of computing collision probability for a collision candidate and N_p is number of particles per marginal. In the case of the optimal map corresponding to the L^p -Wasserstein distance, we have $\beta = \mathcal{O}(nK)$. This becomes possible since the collision probability between i th and j th particle in the k th

marginal is computed using the change in the cost, i.e.,

$$\sum_{l=1, l \neq k}^K \|X_i^{(l)} - X_j^{(k)}\|_p^p + \|X_j^{(l)} - X_i^{(k)}\|_p^p - \|X_i^{(l)} - X_i^{(k)}\|_p^p - \|X_j^{(l)} - X_j^{(k)}\|_p^p.$$

This also implies that the computational complexity with respect to the number of marginals K is $\mathcal{O}(K)$. Overall, we expect Algorithm 1 to have computational complexity of $\mathcal{O}(nK^2N_p)$ for L^p -Wasserstein distance, given K marginals, N_p samples per marginal, and n -dimensional sample space.

- **Low memory consumption.** Since the proposed method does not require computing any distance matrix at any point, which is often used in EMD and Sinkhorn method, it has a more affordable memory consumption of $\mathcal{O}(nKN_p)$ which is of the same order as the input.
- **Relaxed constraints on the cost function.** Our scheme, unlike gradient based methods, does not require regularity conditions on the cost function $c(\cdot)$. In other words, the algorithmic steps of the proposed collision-based dynamics can be performed irrespective of the regularity of $c(\cdot)$. We expect that the proposed method leads to accurate results as long as the original OT problem is well-posed.
- **Constant weight.** In the proposed method, we assumed that the weight of all particles are equal and remain constant in OT problem. This implies that if the input samples are weighted, a resampling method needs to be used to enforce constant weight for all samples. While we see this as a limitation, we believe the proposed numerical scheme may be adapted by the stochastic weighted particle method [37] to allow varying weight to bypass resampling.
- **No data race for collisions in each marginal.** In the collision step for each marginal, the Algorithm 1 tests unique pairs of particles for collisions by construction. Therefore, collisions in each marginals can be trivially parallelized since there is no data race.

6. RESULTS

Here, we test the proposed collision-based Algorithm 1 in solving MMOT to train a multi-marginal sampling model as well as a metric to find distances between images in a dataset. In Appendix B, we carry out further test on several toy problems to validate the convergence rate and computational cost of the proposed method compared to EMD and Sinkhorn. Everywhere in this study, we report an estimate of Wasserstein distance $d^p(\cdot)$ given samples of i the marginal $X^{(i)} \in \mathbb{R}^{N_p \times n}$ for $i = 1, \dots, K$, i.e. $d^p(X) := \sum_{j>k}^K \sum_{i=1}^{N_p} \|X_i^{(j)} - X_i^{(k)}\|_p^p / N_p$. All computations are done on a laptop with an Intel Core i7-8550U CPU that runs with 1.8GHz frequency equipped with 16 GB memory. In this paper we use Python Optimal Transport library [38] for EMD and Sinkhorn computations.

6.1. Learning a five-marginal map

As an interesting application of MMOT, here we deploy the proposed method to learn a map between normal and four other distributions, i.e. Swiss roll, banana, funnel, and ring, see [39] for details.

First, we take $N_p = 2 \times 10^4$ samples from five marginals and construct $X = [X^{(1)}, \dots, X^{(5)}]$ where $X^{(1)} \sim \mathcal{N}(0, I)$ and the other marginals follow density of target densities, i.e. Swiss roll,

banana, funnel, and ring. We find the optimal map between these five marginals using the proposed Algorithm 1. The optimal map provides us with the sampling order which is paired to minimize the transport cost. Then, we train a Neural Network (NN) as a map denoted by $M_{Y \rightarrow Z}$ where the samples of normal distribution $Y := [X^{(1)}]$ is the input and the other marginals $Z := [X^{(2)}, X^{(3)}, X^{(4)}, X^{(5)}]$ are the output. We construct the NN using 4 layers, each with 100 neurons, equipped with $\tanh(\cdot)$ as the activation function and a linear operation at the final layer to set the output dimension to $\dim(Z)$. Here, we use Adam's algorithm [40] with a learning rate of 10^{-3} , take L^2 point-wise error between NN estimate and optimally ordered data as the loss function, and carry out 5,000 iterations to find the NN weights.

For testing, we generate 10^6 normally distributed samples, i.e. $Y^{\text{test}} \sim \mathcal{N}(0, I_{n \times n})$, and feed them as the input into the NN to find $Z^{\text{test}} = M_{Y \rightarrow Z}(Y^{\text{test}})$. As shown in Fig. 1, the estimated map via Neural Network trained using optimally paired samples recovers the target densities with a high accuracy.

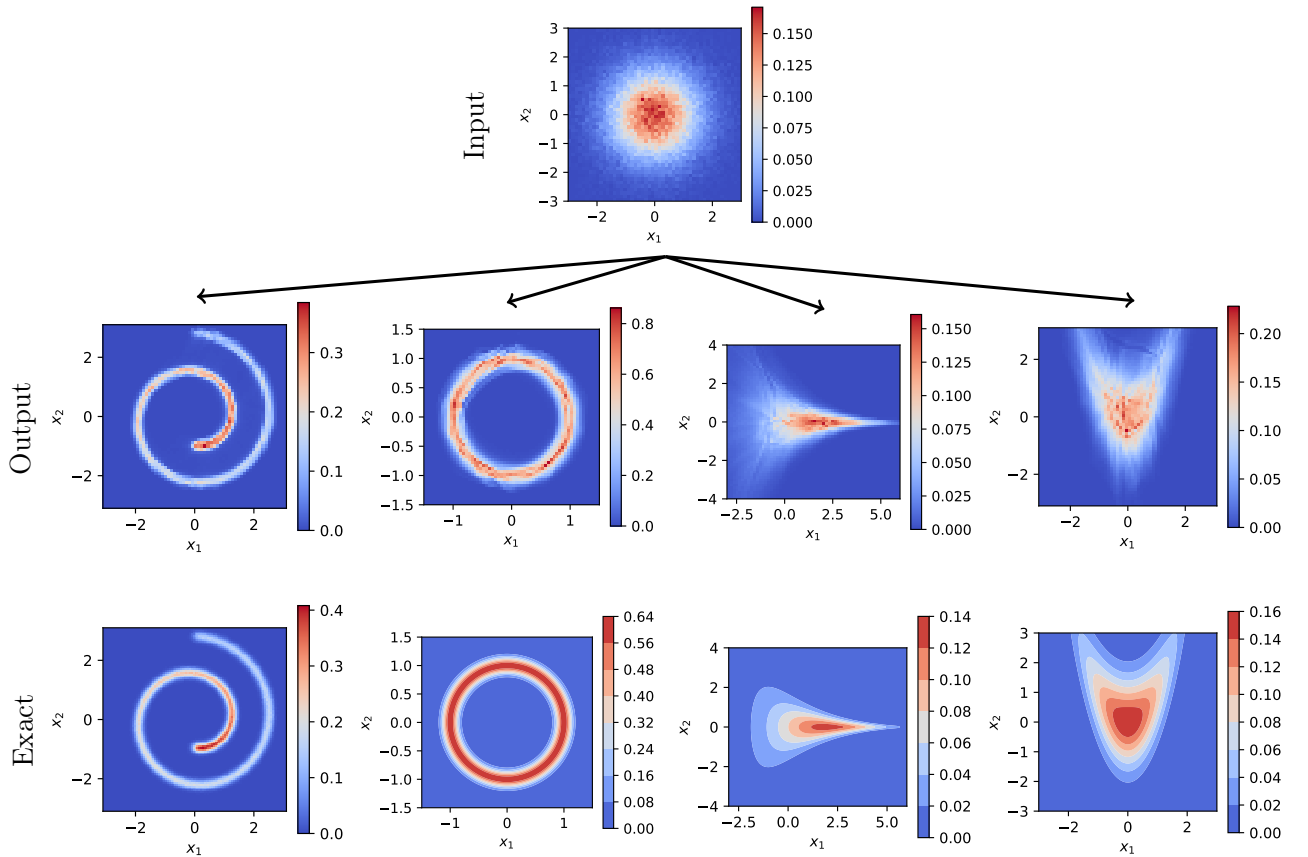


FIGURE 1. Transport map $M_{Y \rightarrow Z}$ based on paired samples of a five-marginal optimal transport problem, i.e. from the normally distributed one-marginal $Y = [X^{(1)}]$ (top) to a four-marginal output $Z = [X^{(2)}, X^{(3)}, X^{(4)}, X^{(5)}]$ (middle and bottom) consisting of the Swiss roll, ring, funnel, and banana distributions.

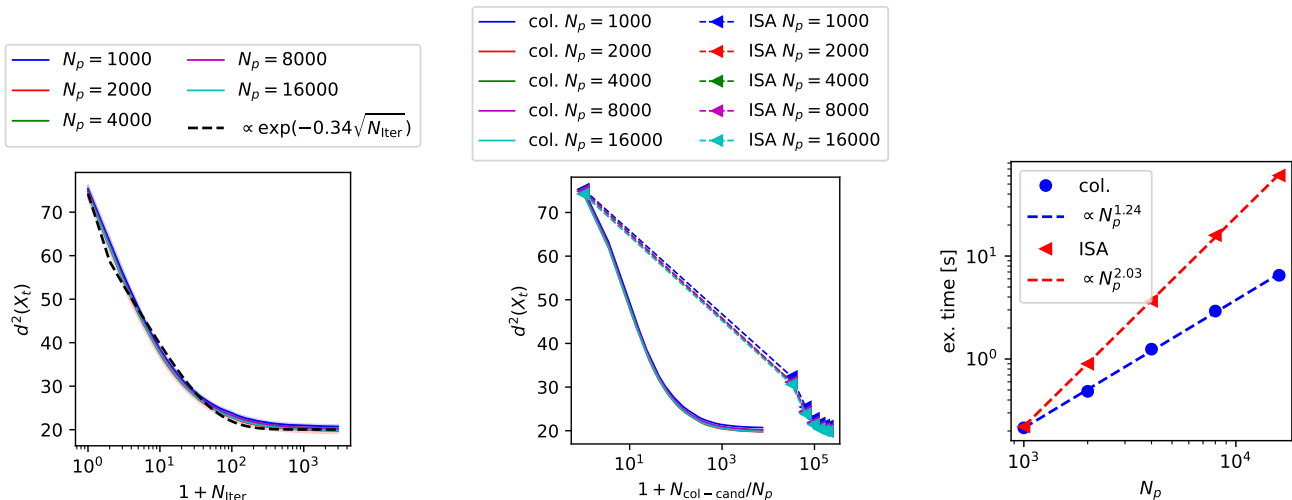


FIGURE 2. Evolution of the cost function during collision-based MMOT Algorithm 1 (left), execution time (middle) and memory consumption (right) for a range of N_p in finding the optimal map between five-marginal consisting of normal, Swiss-roll, banana, ring, funnel densities.

In Fig. 2, we analyze the convergence rate of the proposed algorithm, and its cost with respect to execution time and memory consumption. As expected, we see that Algorithm 1 scales linearly with number of samples, the cost of the optimal map decreases exponentially to its optimal value, and the number of iterations till convergence is not affected by N_p .

Next, we make a comparison between the proposed collision-based OT Algorithm 1 and EMD as well as Sinkhorn method in a two-marginal setting. As an example, let us consider OT problem between normal and Swiss roll distribution. In Fig. 3, we show that the collision-based solution converges to EMD’s solution linearly with the number of iterations. The results also confirm that the computational complexity and the memory consumption of the proposed method scales linearly with N_p which clearly outperforms EMD and Sinkhorn method. For comparison between other two-marginals see Appendix B.

6.2. Distribution of Wasserstein distance in a dataset

One of the applications of Wasserstein distance is labeling datasets, since it provides us with a metric in the space of distributions. Here we show the efficiency of the proposed collision-based solution to MMOT by treating this problem as one. Consider the Japanese Female Facial Expression (JAFFE) [41] and butterfly [42] datasets. The JAFFE dataset consists of 213 images, where we treat each as a marginal. From the butterfly dataset, we consider 50 classes, from which we select 4 pictures randomly which leads to MMOT problem with 200 marginals.

We deploy the collision-based solution Algorithm 1 to these MMOT problems with L^2 -Wasserstein cost to find the pairs of particles/samples across marginals. Since we are minimizing the total cost

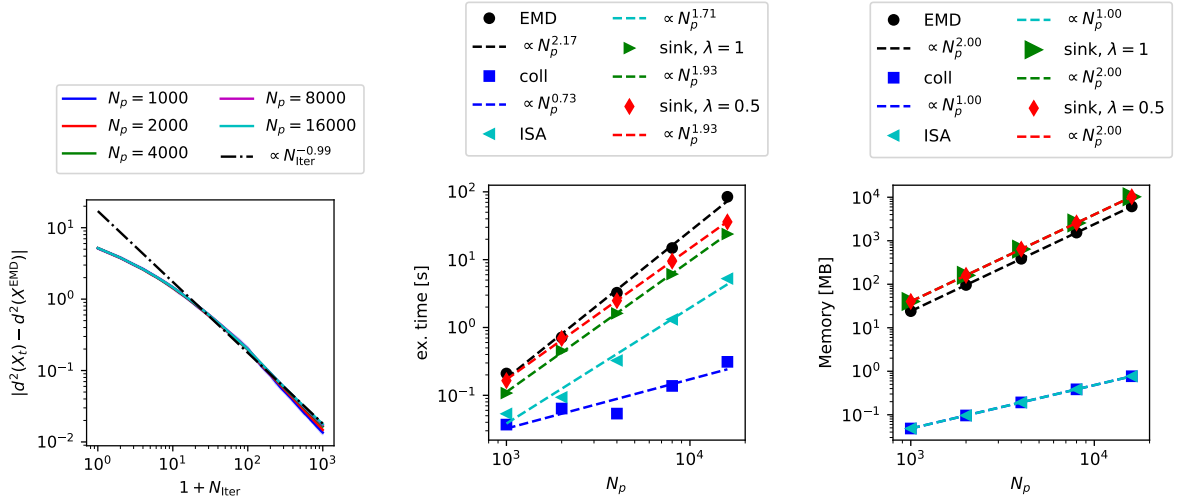


FIGURE 3. Evolution of the error of proposed collision-based MMOT Algorithm 1 from EMD (left), execution time (middle) and memory consumption (right) for a range of N_p in finding optimal two-marginal map between normal and Swiss roll distribution compared to EMD and Sinkhorn with regularization factor $\lambda = 1$ and 0.5 .

$\sum_{j>k}^K \sum_{i=1}^{N_p} \|X_i^{(j)} - X_i^{(k)}\|_2^2 / N_p$, we are also approximating the optimal map between every two j, k marginals that minimizes $\sum_{i=1}^{N_p} \|X_i^{(j)} - X_i^{(k)}\|_2^2 / N_p$.

As shown in Fig. 4-5, the proposed collision MMOT can find the pair-wised Wasserstein distance distribution in both datasets efficiently. We also observe that the convergence rate is not affected by the number of marginals. As expected, the execution time scales $\mathcal{O}(K^2)$ and memory $\mathcal{O}(K)$.

Here, we also compare the solution to optimal transport between two randomly selected pictures (marginals) from JAFFE dataset with the benchmark. As shown in Fig. 6, we observe convergence to the EMD solution with an error of $\epsilon \propto N_{\text{Iter}}^{-1.6}$. Furthermore, we validate the computational complexity reported in section 5, and observe that the proposed collisional OT method outperforms EMD and Sinkhorn with respect to execution time and memory consumption. For further numerical tests, see Appendix B.2.

7. CONCLUSION

We proposed a novel solution algorithm called collision-based dynamics for the discrete OT problem, including multi-marginal settings. The devised collision process is based on random binary swaps of the samples and is built on close analogy with the Boltzmann kinetics. We showed that in the case of L^p -Wasserstein distance, the proposed method has the computational complexity of $\mathcal{O}(nK^2N_p)$, where n is the dimension of each sample, N_p is the number particles/samples per marginal, and K is the number of marginals. We achieved this performance by randomizing the swapping process. The method conserves marginals by construction. We showed empirically that it admits an exponential convergence to a near-optimal solution.

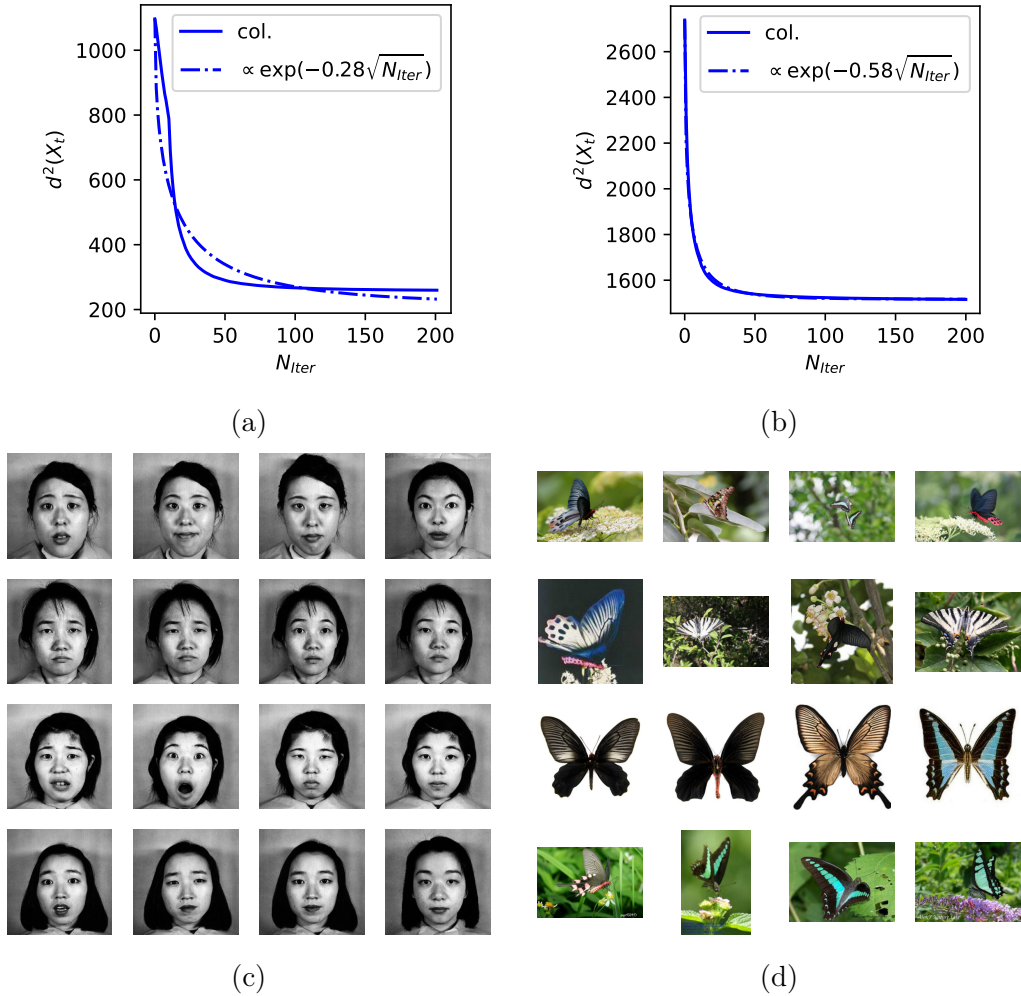


FIGURE 4. Evolution of Wasserstein distance against number of iteration N_{Iter} and $N_{col-cand}$ for collision based OT algorithm 1 (a)-(b) for JAFFE and Butterfly dataset, as well as drawing 4 closest pictures from each dataset for 4 random samples (c)-(d).

We investigated the computational cost, optimality gap, and memory consumption of the collision process in several toy problems, and validated our estimates on the cost and memory requirements. Furthermore, we showed the capability of the proposed method in finding the optimal map in a five-marginal setting. Moreover, we tested the algorithm to find an optimal map between pictures in a dataset, treating it as a multi-marginal OT problem. The proposed collision-based dynamics proves to be highly efficient, e.g., in comparison to the Sinkhorn algorithm. We anticipate broad applications of the devised method in various settings where multi-marginal OT problem is of relevance, including Density Functional Theory [43], among others.

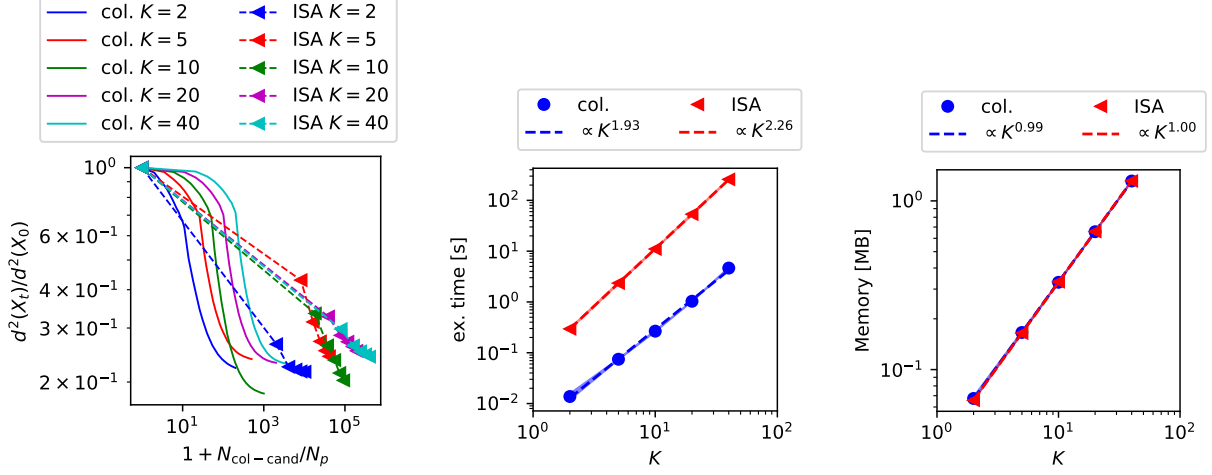


FIGURE 5. Evolution of Wasserstein distance estimate (left), execution time (middle), and memory consumption (right) versus the number of considered marginals for the multi-marginal optimal map problem in JAFFE dataset.

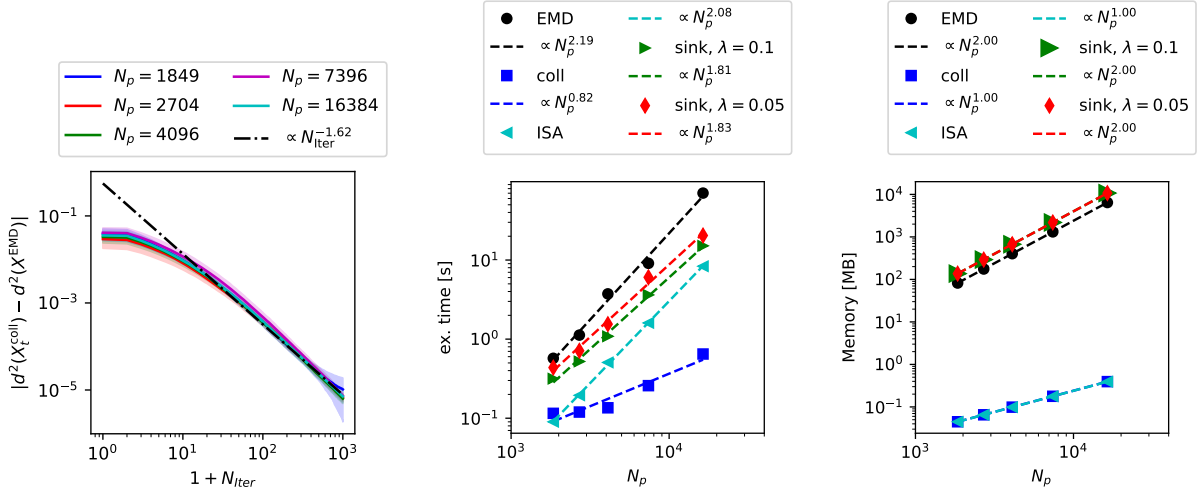


FIGURE 6. Optimal transport between 10 randomly selected pairs of pictures from JAFFE dataset, each for a range of the number of pixels denoted by N_p . Here we investigate the solution from collision-based Algorithm 1 by plotting error from EMD (left), execution time (middle), and memory consumption (right) against EMD and Sinkhorn with a variation of regularization factor λ .

8. ACKNOWLEDGMENT

M. Sadr thanks Andreas Adelmann and Patrick Cheridito for their support and constructive discussions.

REFERENCES

- [1] G. Monge, “Mémoire sur la théorie des déblais et des remblais,” *Mem. Math. Phys. Acad. Royale Sci.*, pp. 666–704, 1781.
- [2] L. Kantorovich, “On the translocation of masses,” *C.R. (Doklady) Acad. Sci. URSS (N.S.)*, vol. 37, pp. 199–201, 1942.
- [3] S. Ferradans, N. Papadakis, G. Peyré, and J.-F. Aujol, “Regularized discrete optimal transport,” *SIAM Journal on Imaging Sciences*, vol. 7, no. 3, pp. 1853–1882, 2014.
- [4] E. Del Barrio, J. A. Cuesta-Albertos, C. Matrán, and A. Mayo-Íscar, “Robust clustering tools based on optimal transportation,” *Statistics and Computing*, vol. 29, pp. 139–160, 2019.
- [5] M. Jacot, V. Champaney, S. T. Jordan, J. Cortial, and F. Chinesta, “Empowering optimal transport matching algorithm for the construction of surrogate parametric metamodel,” *Mechanics & Industry*, vol. 25, p. 9, 2024.
- [6] P. Mohajerin Esfahani and D. Kuhn, “Data-driven distributionally robust optimization using the Wasserstein metric: Performance guarantees and tractable reformulations,” *Mathematical Programming*, vol. 171, no. 1, pp. 115–166, 2018.
- [7] C. Cotar, G. Friesecke, and C. Klüppelberg, “Density functional theory and optimal transportation with Coulomb cost,” *Communications on Pure and Applied Mathematics*, vol. 66, no. 4, pp. 548–599, 2013.
- [8] O. Pele and M. Werman, “Fast and robust earth mover’s distances,” in *2009 IEEE 12th international conference on computer vision*, pp. 460–467, IEEE, 2009.
- [9] N. Bonneel, M. Van De Panne, S. Paris, and W. Heidrich, “Displacement interpolation using Lagrangian mass transport,” in *Proceedings of the 2011 SIGGRAPH Asia conference*, pp. 1–12, 2011.
- [10] M. Cuturi, “Sinkhorn distances: Lightspeed computation of optimal transport,” *Advances in neural information processing systems*, vol. 26, 2013.
- [11] A. Genevay, M. Cuturi, G. Peyré, and F. Bach, “Stochastic optimization for large-scale optimal transport,” *Advances in neural information processing systems*, vol. 29, 2016.
- [12] J.-D. Benamou and Y. Brenier, “A computational fluid mechanics solution to the Monge-Kantorovich mass transfer problem,” *Numerische Mathematik*, vol. 84, no. 3, pp. 375–393, 2000.
- [13] G. Conforti, D. Lacker, and S. Pal, “Projected Langevin dynamics and a gradient flow for entropic optimal transport,” *arXiv preprint arXiv:2309.08598*, 2023.
- [14] M. Sadr, P. M. Esfehiani, and M. H. Gorji, “Optimal transportation by orthogonal coupling dynamics,” *preprint on arXiv:2410.08060*, 2024.
- [15] L. Rüschendorf and S. T. Rachev, “A characterization of random variables with minimum l2-distance,” *Journal of multivariate analysis*, vol. 32, no. 1, pp. 48–54, 1990.
- [16] G. Puccetti, “An algorithm to approximate the optimal expected inner product of two vectors with given marginals,” *Journal of Mathematical Analysis and Applications*, vol. 451, no. 1, pp. 132–145, 2017.
- [17] G. Puccetti, L. Rüschendorf, and S. Vanduffel, “On the computation of Wasserstein barycenters,” *Journal of Multivariate Analysis*, vol. 176, p. 104581, 2020.
- [18] O. Mula and A. Nouy, “Moment-SoS methods for optimal transport problems,” *Numerische Mathematik*, pp. 1–38, 2024.
- [19] M. Sadr, N. G. Hadjiconstantinou, and M. H. Gorji, “Wasserstein-penalized entropy closure: A use case for stochastic particle methods,” *Journal of Computational Physics*, vol. 511, p. 113066, 2024.
- [20] J. Ye, J. Z. Wang, and J. Li, “A simulated annealing based inexact oracle for Wasserstein loss minimization,” in *International Conference on Machine Learning*, pp. 3940–3948, PMLR, 2017.
- [21] N. Bonneel, J. Rabin, G. Peyré, and H. Pfister, “Sliced and Radon Wasserstein barycenters of measures,” *Journal of Mathematical Imaging and Vision*, vol. 51, pp. 22–45, 2015.
- [22] M. Huang, S. Ma, and L. Lai, “A Riemannian block coordinate descent method for computing the projection robust Wasserstein distance,” in *International Conference on Machine Learning*, pp. 4446–4455, PMLR, 2021.
- [23] W. Gangbo and A. Świąch, “Optimal maps for the multidimensional Monge-Kantorovich problem,” *Communications on Pure and Applied Mathematics: A Journal Issued by the Courant Institute of Mathematical Sciences*, vol. 51, no. 1, pp. 23–45, 1998.

- [24] W. Gangbo and R. J. McCann, “The geometry of optimal transportation,” 1996.
- [25] L. A. Caffarelli, “Allocation maps with general cost functions,” in *Partial differential equations and applications*, pp. 29–35, Routledge, 2017.
- [26] L. Nenna, *Numerical methods for multi-marginal optimal transportation*. PhD thesis, Universite Paris sciences et lettres, 2016.
- [27] B. Pass, “Multi-marginal optimal transport: theory and applications,” *ESAIM: Mathematical Modelling and Numerical Analysis*, vol. 49, no. 6, pp. 1771–1790, 2015.
- [28] C. Villani *et al.*, *Optimal transport: old and new*, vol. 338. Springer, 2009.
- [29] M. Thorpe, “Introduction to optimal transport,” *Notes of Course at University of Cambridge*, 2018.
- [30] J. Cuesta-Albertos, C. Matrán, and A. Tuero-Diaz, “Optimal transportation plans and convergence in distribution,” *Journal of multivariate analysis*, vol. 60, no. 1, pp. 72–83, 1997.
- [31] H. W. Kuhn, “The Hungarian method for the assignment problem,” *Naval research logistics quarterly*, vol. 2, no. 1-2, pp. 83–97, 1955.
- [32] G. A. Bird, “Approach to translational equilibrium in a rigid sphere gas,” *Physics of Fluids*, vol. 6, no. 10, 1963.
- [33] J.-G. Liu and Y. Wang, “On random batch methods (RBM) for interacting particle systems driven by Levy processes,” *arXiv preprint arXiv:2412.06291*, 2024.
- [34] W. Wagner, “A convergence proof for Bird’s direct simulation Monte Carlo method for the Boltzmann equation,” *Journal of Statistical Physics*, vol. 66, pp. 1011–1044, 1992.
- [35] G. A. Bird, *Molecular gas dynamics and the direct simulation of gas flows*. Clarendon Press, 1994.
- [36] T. Takizuka and H. Abe, “A binary collision model for plasma simulation with a particle code,” *Journal of computational physics*, vol. 25, no. 3, pp. 205–219, 1977.
- [37] S. Rjasanow and W. Wagner, “A stochastic weighted particle method for the Boltzmann equation,” *Journal of Computational Physics*, vol. 124, no. 2, pp. 243–253, 1996.
- [38] R. Flamary, N. Courty, A. Gramfort, M. Z. Alaya, A. Boisbunon, S. Chambon, L. Chapel, A. Corenflos, K. Fatras, N. Fournier, L. Gautheron, N. T. Gayraud, H. Janati, A. Rakotomamonjy, I. Redko, A. Rolet, A. Schutz, V. Seguy, D. J. Sutherland, R. Tavenard, A. Tong, and T. Vayer, “POT: Python Optimal Transport,” *Journal of Machine Learning Research*, vol. 22, no. 78, pp. 1–8, 2021.
- [39] R. Baptista, Y. Marzouk, and O. Zahm, “On the representation and learning of monotone triangular transport maps,” *Foundations of Computational Mathematics*, pp. 1–46, 2023.
- [40] D. P. Kingma, “Adam: A method for stochastic optimization,” *arXiv preprint arXiv:1412.6980*, 2014.
- [41] M. J. Lyons, S. Akamatsu, M. Kamachi, J. Gyoba, and J. Budynek, “The Japanese female facial expression (JAFFE) database,” in *Proceedings of third international conference on automatic face and gesture recognition*, pp. 14–16, 1998.
- [42] T. Chen, W. Wu, Y. Gao, L. Dong, X. Luo, and L. Lin, “Fine-grained representation learning and recognition by exploiting hierarchical semantic embedding,” in *Proceedings of the 26th ACM international conference on Multimedia*, pp. 2023–2031, 2018.
- [43] G. Buttazzo, L. De Pascale, and P. Gori-Giorgi, “Optimal-transport formulation of electronic density-functional theory,” *Physical Review A—Atomic, Molecular, and Optical Physics*, vol. 85, no. 6, p. 062502, 2012.
- [44] Y. LeCun, C. Cortes, and C. Burges, “Mnist handwritten digit database,” *ATT Labs [Online]*. Available: <http://yann.lecun.com/exdb/mnist>, vol. 2, 2010.

APPENDIX A. ITERATED SWAPPING ALGORITHM

Here, we give a short description of ISA algorithm used in this paper, given its similarity to the collision-based method proposed in this paper. As detailed in Algorithm 2, in each iteration for each marginal, $\mathcal{O}(N_p^2)$ operations are carried out, while each particle maybe be accepted for swap (collision) more than once. This makes the algorithm prone to data race as an issue for shared-memory parallelism.

Algorithm 2: Iterated Swapping Algorithm for the MMOT problem

Input: $X := [X^{(1)}, \dots, X^{(K)}]$ and tolerance $\hat{\epsilon}$ $\# \dim(X) = K \times N_p \times n$

repeat

for $i = 1, \dots, K$ **do**

for $j = 1, \dots, N_p$ **do**

for $k = j + 1, \dots, N_p$ **do**

if $\sigma(X_j^{(i)}, X_k^{(i)}; X_k^{(i)}, X_j^{(i)}) = 1$ **then**

$\#$ Accept the collision and update X ;

$X_j^{(i)} \leftarrow X_k^{(i)}$ and $X_k^{(i)} \leftarrow X_j^{(i)}$;

end

end

end

end

end

until Convergence in $\mathbb{E}_{\hat{\pi}_t}[c(X_t)]$ with tolerance $\hat{\epsilon}$;

Output: X

APPENDIX B. FURTHER RESULTS

In this section, we test the convergence rate of the proposed collision-based solution algorithm to the optimal transport problem in several toy problems.

B.1. Optimal map between two n -dimensional random Gaussians

In this section, we consider two-marginal random Gaussian distributions as a complicated toy problem. Consider random variables $X^{(1)}$ and $X^{(2)}$ that are sampled via

$$X_i^{(1)} \sim \mathcal{N}(\mu_i^{(1)} \mathbf{1}_n, \sigma_i^{(1)} I_{n \times n}), \quad (17)$$

$$X_i^{(2)} \sim \mathcal{N}(\mu_i^{(2)} \mathbf{1}_n, \sigma_i^{(2)} I_{n \times n}), \quad (18)$$

where

$$\mu_i^{(1)}, \mu_i^{(2)} \sim \mathcal{U}([-10, 10]), \quad (19)$$

$$1/\sigma_i^{(1)}, 1/\sigma_i^{(2)} \sim \Gamma(3, 1), \quad (20)$$

for $i = 1, \dots, N_p$. Here, $\mathbf{1}_n$ denotes a n -dimensional unit vector, $\mathcal{U}([a, b])$ is a uniform distribution on $[a, b]$, $\Gamma(\alpha, \theta)$ is the Gamma distribution with the shape parameter α and the scale parameter

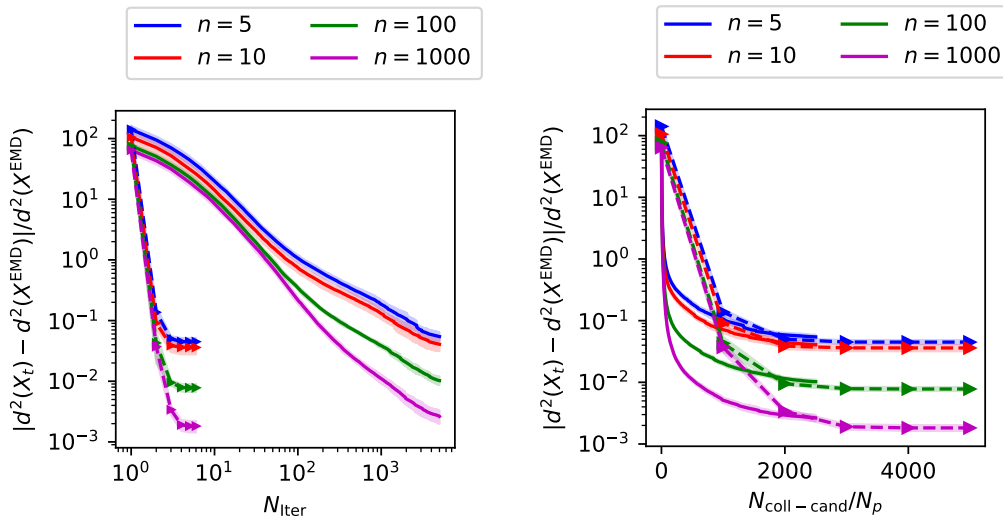


FIGURE 7. Relative error in Wasserstein distance against the dimension of two random variables that follow random Gaussian distribution for a range of dimension $n = 5, 10, 100, 1000$ described in B.1. Solution of algorithm 1 is shown in solid lines, and ISA with dashed lines with \blacktriangleright symbol

θ . Given samples of $X^{(1)}$ and $X^{(2)}$, we would like to find the optimal map between them that minimizes $\sum_{i=1}^{N_p} \|X_i^{(1)} - X_i^{(2)}\|_2^2 / N_p$. This toy problem allows us to create samples of a complicated n -dimensional distribution, which we use to analyze the proposed collision-based OT algorithm 1 compared to the benchmark.

In Fig. 7, we compare the relative error between EMD and the solution obtained from collision-based OT algorithm 1 in estimating the L^2 -Wasserstein distance for a range of $n = 5, 10, 100, 1000$. Clearly, by increasing n , the relative error of collisional OT from EMD is reduced. Here, we also make comparison to the standard ISA algorithm, where we show that the proposed collision-based algorithm achieves reasonable relative error with less number of collision candidates.

B.2. Wasserstein distance in several datasets

As an example from image processing, here we consider optimal transport problem given data from standard datasets such as JAFFE, butterfly, and MNIST [44]. In each case, we take 100 random pairs of pictures from the dataset, and find the optimal map between them using EMD, Sinkhorn, and the proposed collision-based OT Algorithm 1. As shown in Fig. 9, the proposed collision-based approach outperforms Sinkhorn in the distribution of relative error in Wasserstein distance, speed-up and memory consumption.

B.3. Optimal map between normal and Swiss roll/banana/funnel/ring density

Consider two-marginal optimal map between normal distribution $\mu_1 = \mathcal{N}(0, I_{2 \times 2})$ and a target distribution μ_2 . Here, we consider Swiss roll, banana, funnel, and ring as target densities, see [39] for

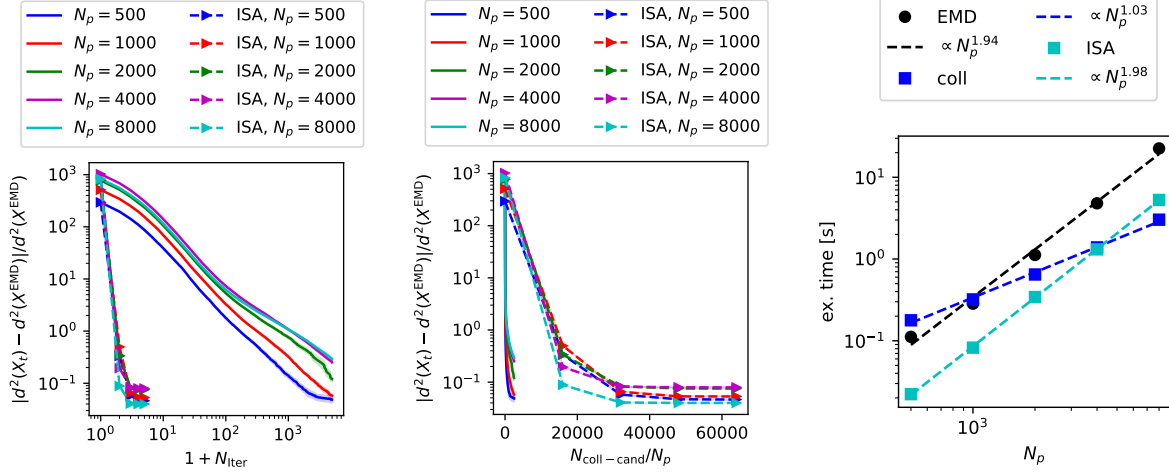


FIGURE 8. Relative error in Wasserstein distance against N_p of two random variables that follow random Gaussian distribution with $n = 2$ described in B.1.

details. We draw N_p samples from the two marginals, and solve the optimal transport problem using the proposed collision-based algorithm 1, EMD and Sinkhorn. As shown in Fig. 10, the proposed algorithm outperforms the benchmark at a reasonable error, both in terms of execution time and memory consumption.

B.4. Coloring images

Assume we are given a picture of Robert De Niro¹ in gray and color. We intend to learn the map between the colored and black/white pictures and use it to turn another black/white picture into a colorful one. We take 4,000 samples from De Niro’s picture, use the collision-based algorithm to find the optimal map on discrete points and train a NN denoted by M with L^2 -pointwise error between optimally sorted data points and NN prediction as loss. We construct the NN using 4 layers, each with 100 neurons, equipped with $\tanh(\cdot)$ as activation function and use Adam’s algorithm [40] with a learning rate of 10^{-3} , take L^2 point-wise error between NN estimate and optimally ordered data as the loss function, and carry out 5,000 iterations to find the NN weights. Afterward, we test NN by plugging in a black/white portrait of Albert Einstein² as input and recover a colored picture as the output, see Fig. 11.

¹This image is taken from the public domain available on commons.wikimedia.org/wiki/File:Robert_De_Niro_KVIFFF_portrait.jpg.

²This image is taken from the public domain available on commons.wikimedia.org/wiki/File:Three_famous_physicists.png.

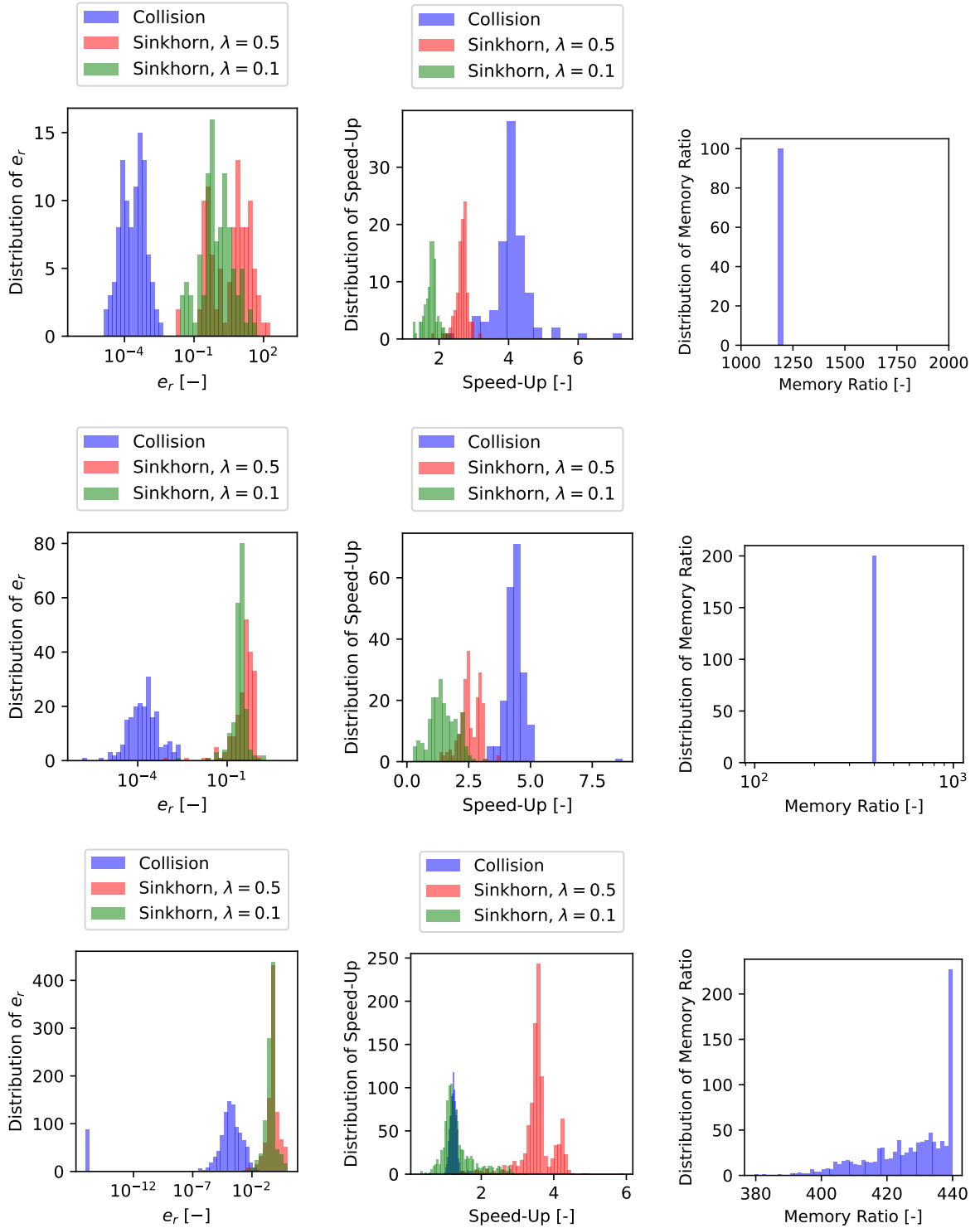


FIGURE 9. Distribution of relative error $e_r := |d^2(X^{\text{coll}}) - d^2(X^{\text{EMD}})|/d^2(X^{\text{EMD}})$ (left), speed-up, i.e. ratio of EMD execution time to collision method (middle), and ratio of memory consumption, i.e. EMD to collision method, (right) for 100 randomly selected pairs of picture from JAFFE (top), butterfly (middle), and MNIST (bottom) dataset with 2,000, 2,000, and 28^2 pixel images.

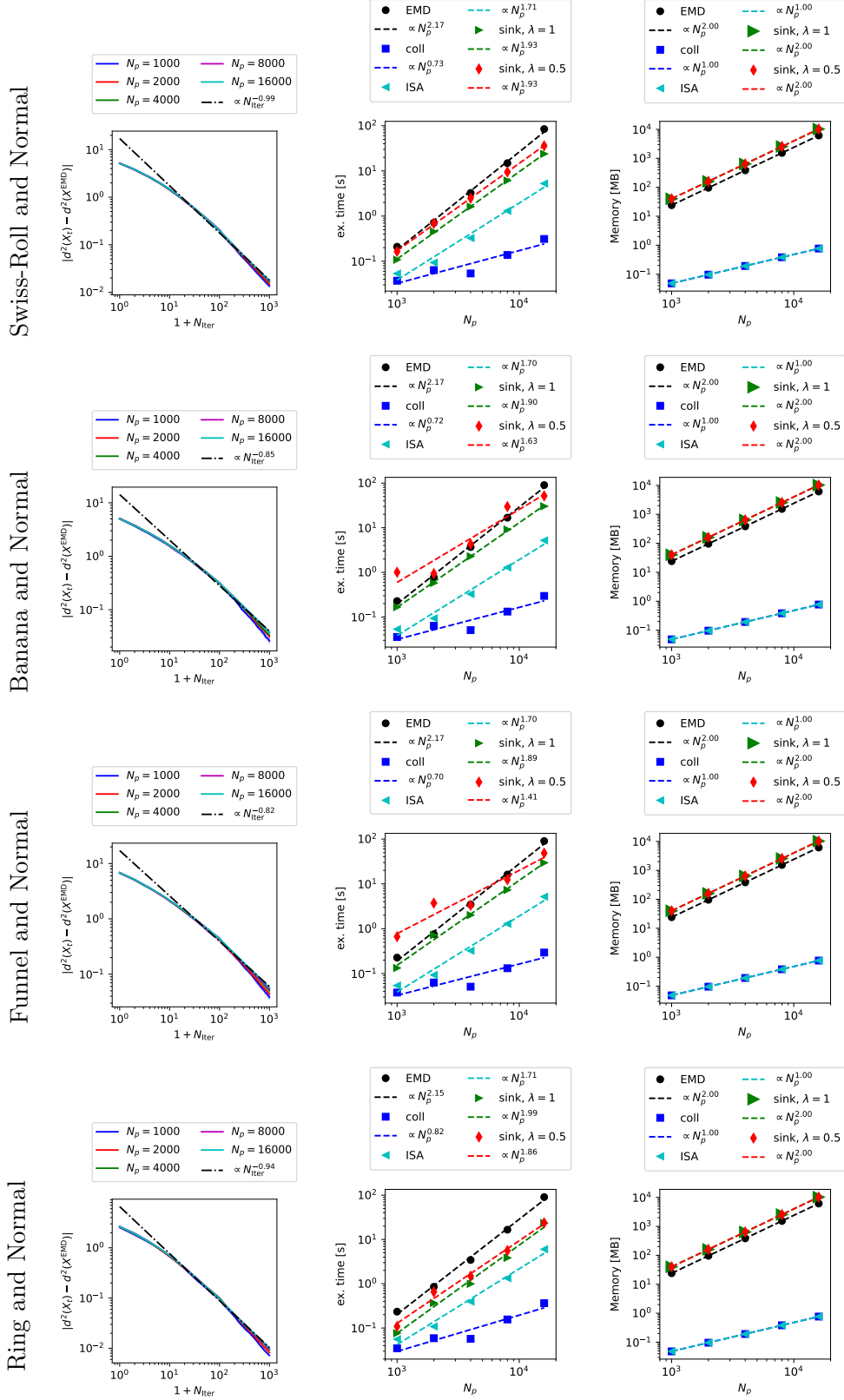


FIGURE 10. Error in the Wasserstein distance $d^2(\cdot, \cdot)$ between the proposed collision-based solution algorithm and EMD (left) execution time (middle) and the memory consumption (right) against the number of particles N_p compared to EMD and Sinkhorn with regularization factor λ .

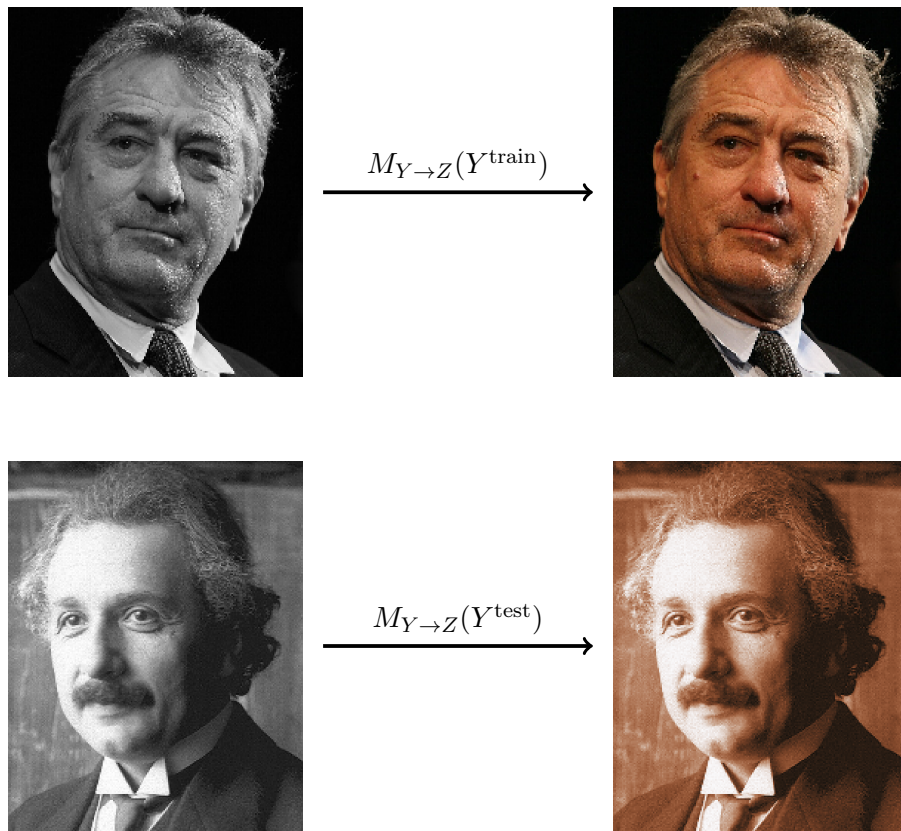


FIGURE 11. After training a network to learn the map $M_{Y \rightarrow Z}$ on the optimally paired data of gray and colored portrait of Robert De Niro (top), we test the network to find a colored picture of Einstein given a gray portrait of him (bottom).